HOKKAIDO UNIVERSITY

Title	Blocking of oestrogen signals improves anti-tumour effect regardless of oestrogen receptor alpha expression in cancer cells
Author(s)	Kajihara, Nabeel; Ge, Yunqi; Seino, Ken-ichiro
Citation	British journal of cancer, 129(6), 935-946 https://doi.org/10.1038/s41416-023-02381-0
Issue Date	2023-10-05
Doc URL	https://hdl.handle.net/2115/93015
Rights	This version of the article has been accepted for publication, after peer review (when applicable) and is subject to Springer Nature's AM terms of use, but is not the Version of Record and does not reflect post-acceptance improvements, or any corrections. The Version of Record is available online at: http://dx.doi.org/10.1038/s41416-023-02381-0
Type	journal article
File Information	72134_3_supp_873177_rxm23m.pdf, Supplementary figure

Hokkaido University Collection of Scholarly and Academic Papers : HUSCAP

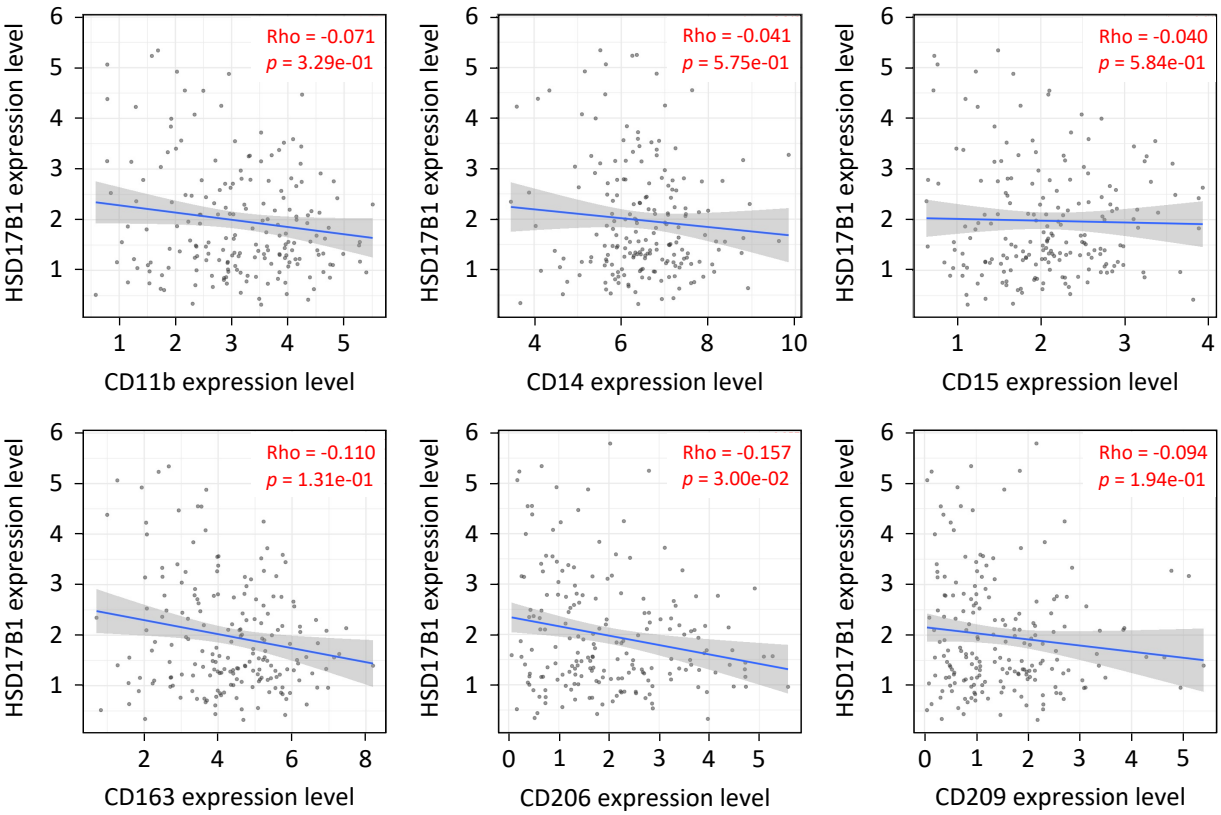


Fig. S1 The association between HSD17B1 and myeloid cell-related genes within human TNBC tumors.
Spearman correlation coefficient between relative HSD17B1 and CD11b, CD14, CD15, CD163, CD206, and CD209 expression in TNBC tumors are shown (n=159).

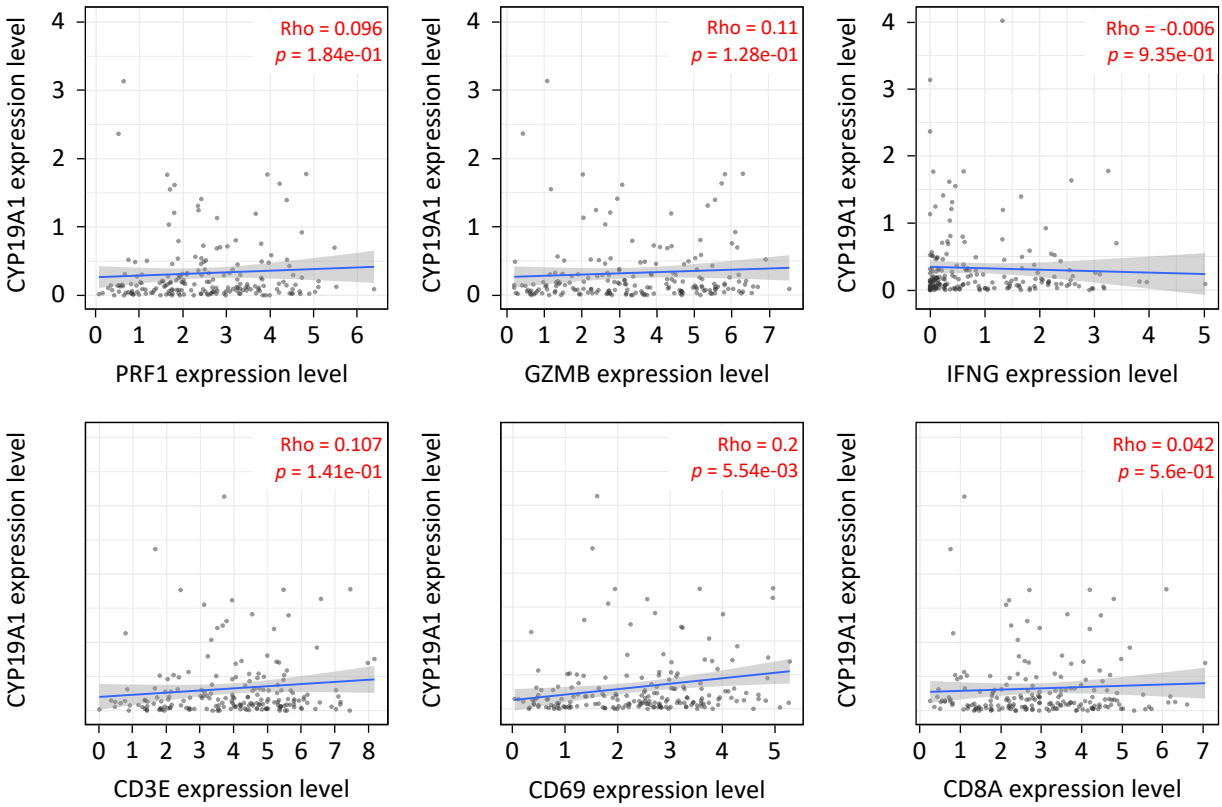


Fig. S2 The association between CYP19A1 and effector lymphocyte-related genes within human TNBC tumors.
Spearman correlation coefficient between relative CYP19A1 and PRF1, GZMB, IFNG, CD3E, CD69, and CD8A expression in TNBC tumors are shown (n=159).

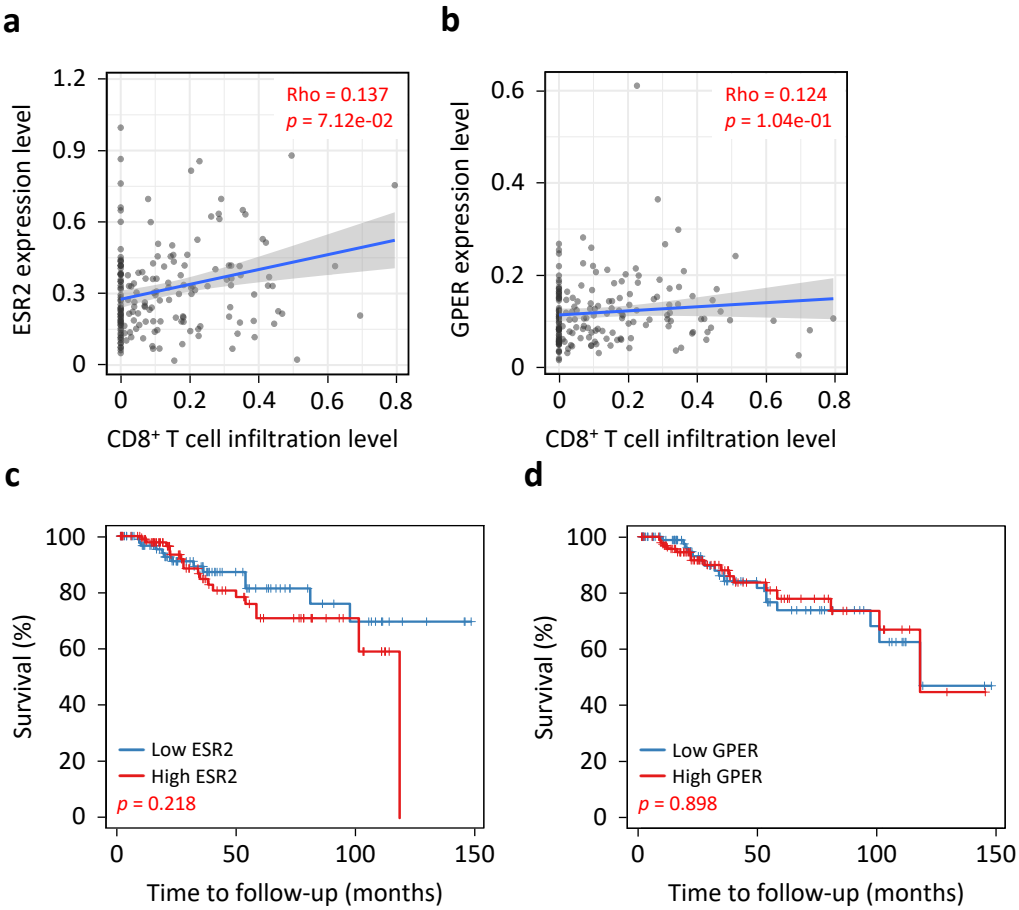


Fig. S3 Potential involvement of ESR2 or GPER with CD8⁺ T cells and a prognosis in human TNBC.
(a, b) Spearman correlation coefficient between relative ESR2/GPER expression in tumors and intra-tumoral CD8⁺ T cell infiltration is shown. (c, d) Kaplan-Meier plot of overall survival of TNBC patients with high or low ESR2/GPER expression. Values were analyzed by a Log-rank test (c, d).

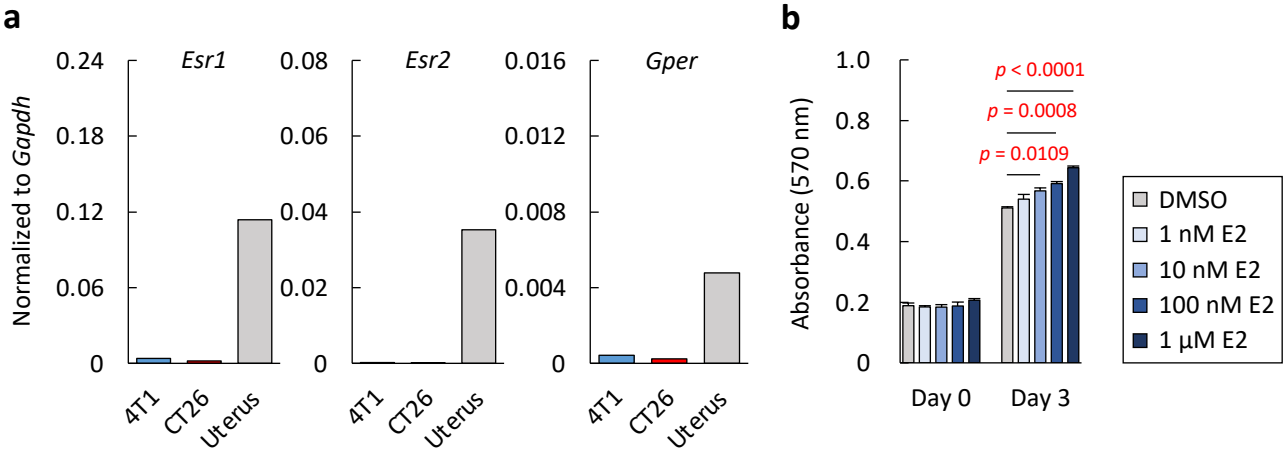


Fig. S4 Expression of ESR2 and GPER in 4T1 or CT26 and estrogen (E2) effects on T47D proliferation *in vitro*.
(a) Bar graphs represent the gene expression of *Esr1*, *Esr2*, and *Gper* in 4T1 or CT26 cells (n=3). Uterus served as a positive control. Gene expression levels were determined by RT-PCR, as normalized to *Gapdh*. (b) Bar graphs represent cell proliferation of T47D cells at varying concentrations of E2 that were measured by MTT assay on day 3 (n=3). Values were analyzed by a Tukey-Kramer test and are shown as mean ± SEM.

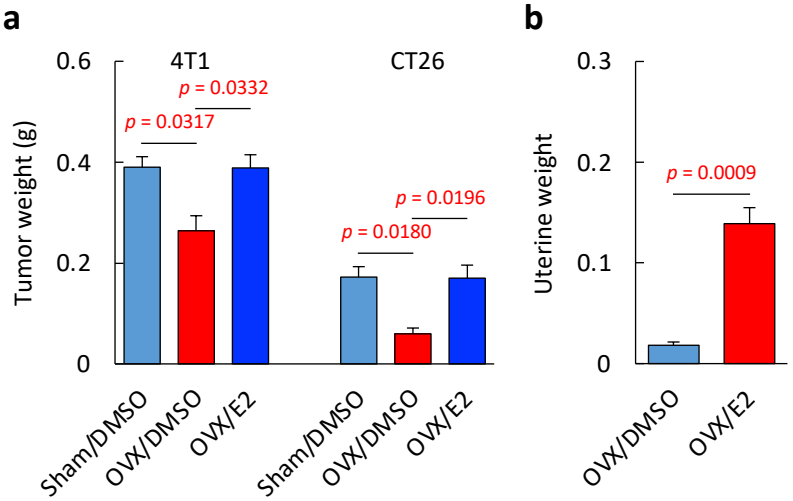


Fig. S5 Effects of estrogen on tumor volume in ERα-negative cancers.
(a) 4T1 or CT26 cells (1x10^5 cells) were subcutaneously inoculated into BALB/c sham-operated (Sham) or ovariectomized (OVX) mice and supplemented with dimethyl sulfoxide (DMSO) or E2. Bar graphs represent the harvested tumor weight from Sham or OVX mice supplemented with DMSO or E2 for 14 days after tumor development (n=4-6). (b) Bar graphs represent the harvested uterine weight from OVX mice supplemented with DMSO or E2 for 14 days after tumor development (n=3). Values were analyzed by a Tukey-Kramer test (a), a two-sided Student's *t*-test (b), and are shown as mean ± SEM.

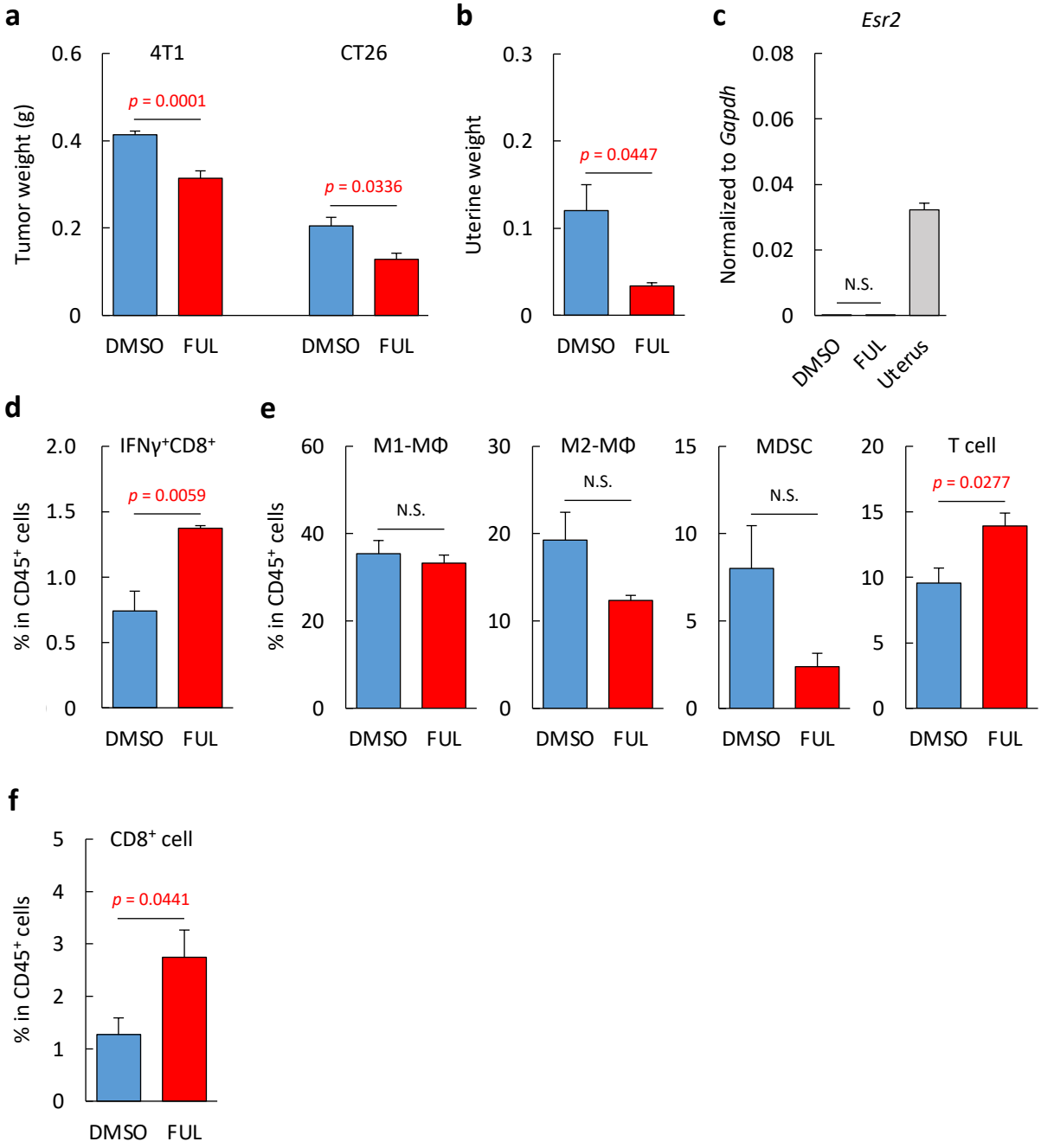


Fig. S6 Effects of fulvestrant on tumor weight and TME in ERα-negative cancers.
(a) 4T1 or CT26 cells (1x10^5 cells) were subcutaneously inoculated into BALB/c mice and treated with dimethyl sulfoxide (DMSO) or fulvestrant (FUL). Bar graphs represent the harvested tumor weight from mice treated with DMSO or FUL for 14 days after tumor development (n=6-8). (b) Bar graphs represent the harvested uterine weight from mice treated with DMSO or FUL for 14 days after tumor development (n=3). (c) Bar graphs represent the gene expression of *Esr2* in 4T1 tumors (n=3). Uterus served as a positive control. Gene expression levels were determined by RT-PCR, as normalized to *Gapdh*. (d) Bar graphs represent the frequency of interferon-γ$^+$CD8$^+$ T cells (CD3$^+$CD8$^+$IFNg$^+$ cells) within CD45$^+$ cells infiltrated in the 4T1 tumors (n=4). (e) Bar graphs represent the frequency of M1-macrophage (M1-MΦ, CD11b$^+$F4/80$^+$CD69$^+$ cells), M2-macrophage (M2-MΦ, CD11b$^+$F4/80$^+$CD206$^+$ cells), myeloid-derived suppressor cell (MDSC, CD11b$^+$Ly6C^{lo}Ly6G$^+$ cells), and T cell (CD3$^+$ cells) within CD45$^+$ cells infiltrated in the CT26 tumors (n=4). (f) Bar graphs represent the frequency of CD8$^+$ T cell (CD3$^+$CD8$^+$ cells) within CD45$^+$ cells infiltrated in the CT26 tumors (n=4). Values were analyzed by a two-sided Student's *t*-test and are shown as mean ± SEM.

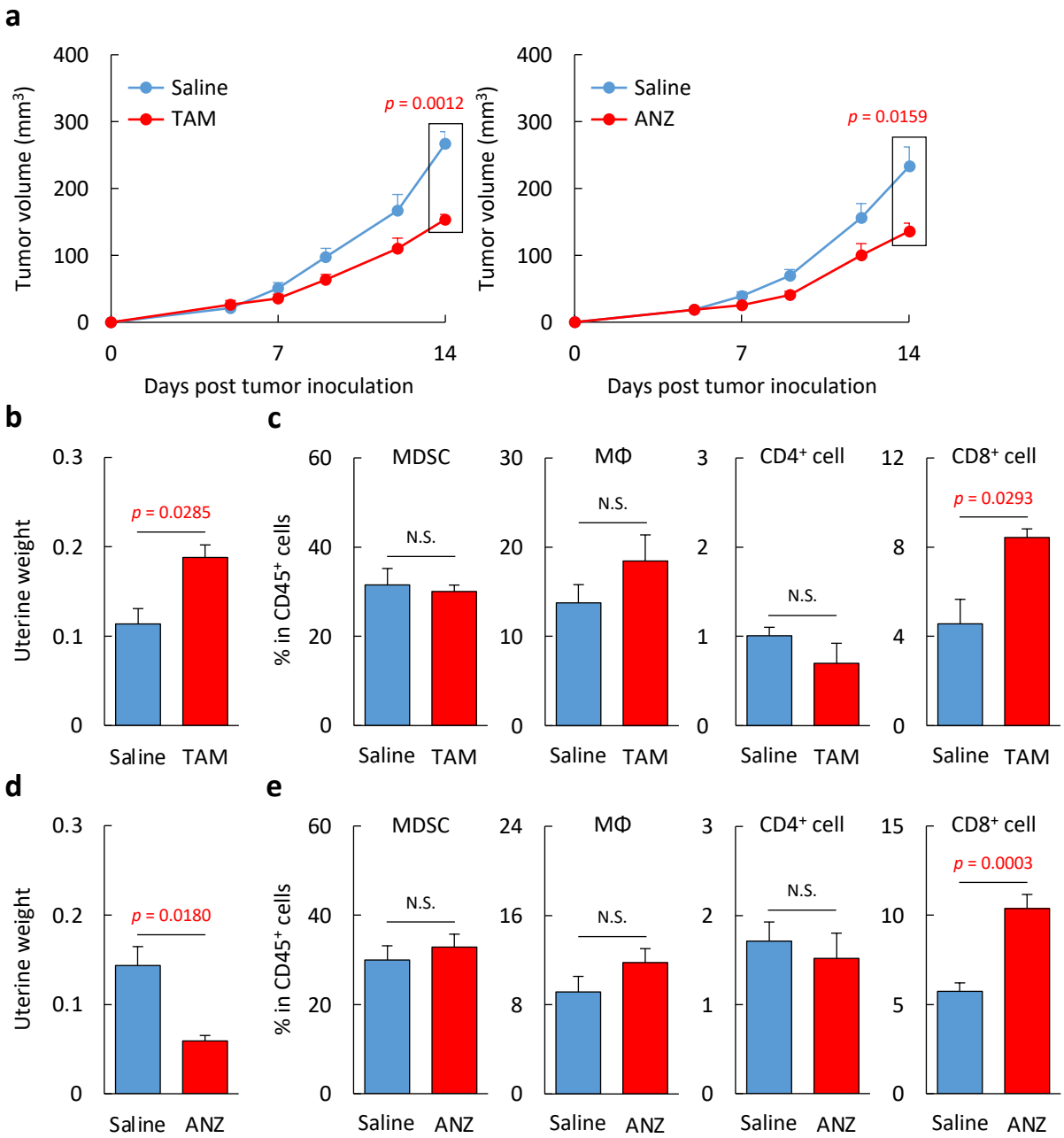


Fig. S7 Effects of anti-estrogenic therapies (tamoxifen or anastrozole) on tumor growth and TME in ERα-negative cancers.

(a) Subcutaneous tumor growth in BALB/c mice inoculated with 4T1 cells ($1x10^5$ cells, n=4-6) and treated with tamoxifen (TAM) or anastrozole (ANZ). (b, d) Bar graphs represent the harvested uterine weight from mice treated with Saline, TAM, or ANZ for 14 days after tumor development (n=3). (c, e) Bar graphs represent the frequency of myeloid-derived suppressor cell (MDSC, $CD11b^+Ly6C^{lo}Ly6G^+$ cells), macrophage (MΦ, $CD11b^+F4/80^+$ cells), $CD4^+$ T cell ($CD3^+CD4^+$ cells), and $CD8^+$ T cell ($CD3^+CD8^+$ cells) within $CD45^+$ cells infiltrated in the 4T1 tumors (n=4-6). Values were analyzed by a two-sided Student's *t*-test and are shown as mean ± SEM.

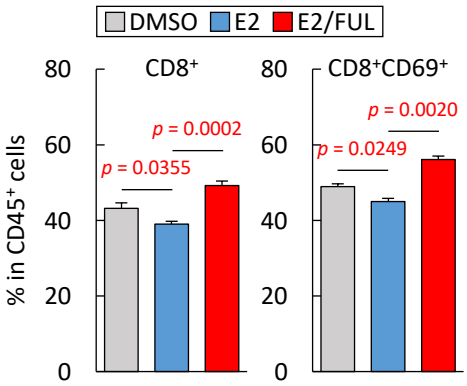


Fig. S8 Effects of estrogen (E2) on mouse CD8$^+$ T cells *in vitro*.
CD8$^+$ T cells were isolated from mouse splenocytes and cultured with DMSO or E2 (1 μM) or E2 (1 μM) combined with FUL (10 μM) for four days. Bar graphs represent the frequency of CD8$^+$ and CD8$^+$CD69$^+$ T cells within CD45$^+$ cells (n=3). Values were analyzed by a Tukey-Kramer test and are shown as mean ± SEM.

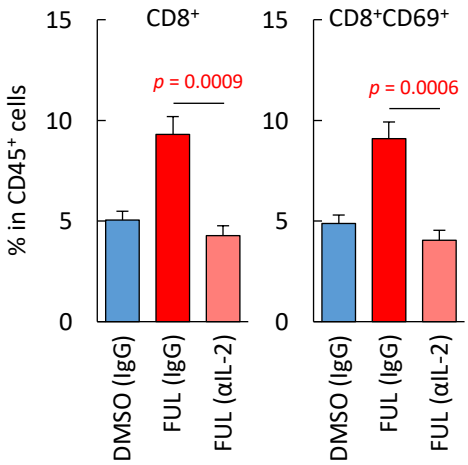


Fig. S9 Effects of anti-IL-2 antibody administration on tumor-infiltrating CD8$^+$ T cells in ERα-negative cancer.
4T1 cells (1x10^5 cells) were subcutaneously inoculated into BALB/c mice and treated with dimethyl sulfoxide (DMSO) or fulvestrant (FUL) combined with IgG or anti-IL-2 antibody (αIL-2). Bar graphs represent the frequency of CD8$^+$ and CD8$^+$CD69$^+$ T cells within CD45$^+$ cells infiltrated in the 4T1 tumors (n=4). Values were analyzed by a Tukey-Kramer test and are shown as mean ± SEM.

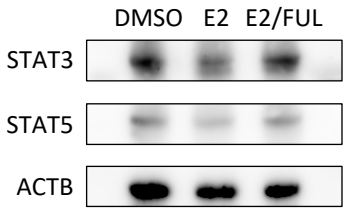


Fig. S10 Effects of estrogen (E2) on STAT signaling in mouse CD8$^+$ T cells *in vitro*.
CD8$^+$ T cells were isolated from mouse splenocytes and cultured with DMSO or E2 or E2 combined with FUL for four days. Western blotting of STAT3 and 5 in CD8$^+$ T cells. ACTB expression was used as an internal control.

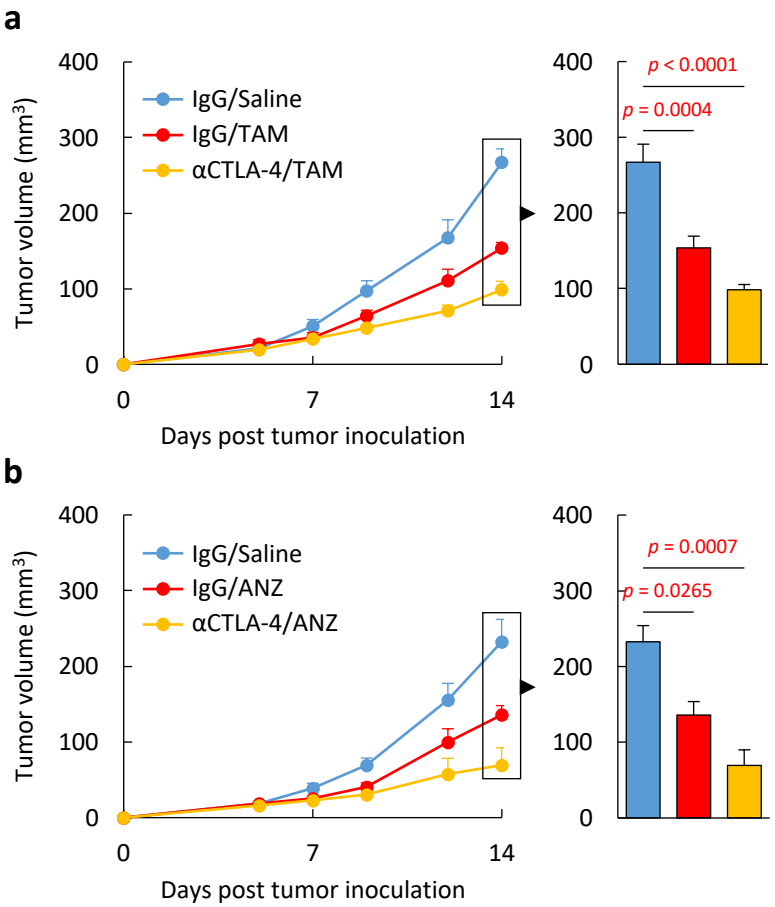


Fig. S11 Effects of anti-estrogenic therapies (tamoxifen or anastrozole) combined with immune checkpoint inhibitor on ERα-negative tumor growth.

(a, b) Subcutaneous tumor growth in BALB/c mice inoculated with 4T1 cells ($1x10^5$ cells, n=3-5) and treated with tamoxifen (TAM) or anastrozole (ANZ) and anti-CTLA-4 antibody (αCTLA-4). Bar graphs represent each group's tumor volume 14 days post tumor development. Values were analyzed by a Tukey-Kramer test and are shown as mean ± SEM.